American Journal of Materials Science and Engineering, 2024, Vol. 12, No. 2, 30-34
Available online at http://pubs.sciepub.com/ajmse/12/2/2
Published by Science and Education Publishing
DOI:10.12691/ajmse-12-2-2

Effect of Grain Size on Spectral Response and Eternal Quantum Efficiency of a Polycrystalline Bifacial Silicon Solar Cell

Adama NDIAYE[1,*], Amadou DIAO[1], Mountaga BOIRO[1], Ibrahima TOURE[1], Senghane MBODJI[2]

[1]Semiconductors and Solar Energy Laboratory, Department of Physics, Faculty of Sciences and Techniques, Cheikh Anta Diop University, Dakar / Senegal
[2]Research Team in Renewable Energies, Materials and Laser, Department of Physics, UFR SATIC, Alioune Diop University, Bambey / Senegal
*Corresponding author: ndiayadama21@gmail.com

Received August 14, 2024; Revised September 16, 2024; Accepted September 22, 2024

Abstract In this work, a 3D theoretical study of a grain columnar model of a bifacial silicon solar cell under monochromatic illumination, is done. From the continuity equation of the photocreated minority carriers in the base of the cell, we determined the expression of the minority carriers' density according to the wavelength, the grain size, the recombination velocity at grain boundaries and the recombination velocities at the junction and the rear side. By the use of the minority carriers' density, the expressions of the photocurrent density, the spectral response and the external quantum efficiency have been deduced. We noted an improvement in spectral response and quantum efficiency with the increase of the grain size. Although, the recombination velocity at the grain boundaries leads to a decrease in spectral response and quantum efficiency; what corresponds to a poor quality of the solar cell since there is a degradation of its intrinsic properties.

Keywords: *bifacial photocell, grain size, wavelength, spectral response, quantum efficiency*

Cite This Article: Adama NDIAYE, Amadou DIAO, Mountaga BOIRO, Ibrahima TOURE, and Senghane MBODJI, "Effect of Grain Size on Spectral Response and Eternal Quantum Efficiency of a Polycrystalline Bifacial Silicon Solar Cell." *American Journal of Materials Science and Engineering*, vol. 12, no. 2 (2024): 30-34. doi: 10.12691/ajmse-12-2-2.

1. Introduction

The efficiency of solar cells is an important factor in optimizing photovoltaic energy. The energy conversion efficiency of photovoltaic panels supplied on the market is around 26%. In addition, this conversion efficiency depends on the weather conditions, the technology used to manufacture the solar cells, their intrinsic properties and the installation technique of the photovoltaic systems [1]. Thus, a few characterization techniques have been developed in order to improve the energy conversion efficiency of solar cells. By means of appropriate methods across different regimes, some researchers worked, in quasi-static state, on the quantum efficiency with or without an applied magnetic field [2], the electrical parameters [3,4] and electronic parameters of a 3D solar cell [5,6,7,8,9]. Other researchers have developed, in transient regime [10], a few techniques for characterizing some electrical parameters and then in frequency modulation [11] of solar cells.

2. Theory

We consider a 3D cubic model of a bifacial solar cell of a n+-p-p+ type [12,13,14,15] in figure 1:

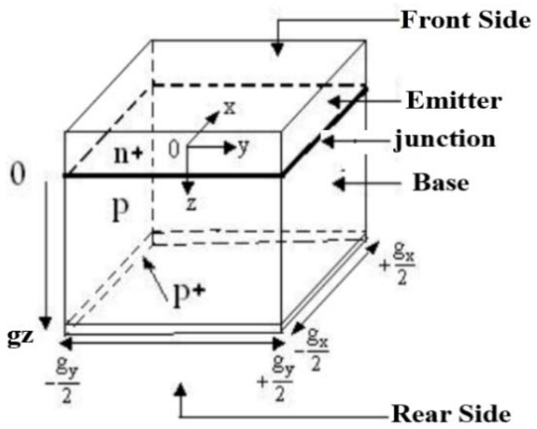

Figure 1. Schematic model of a 3D bifacial silicon solar cell

Where gz is the thickness of the grain; gx and gy are the thicknesses of the grain along the (ox) and (oy) axes respectively.In this study, the contribution of the emitter is neglected, we only take into account that of the base [12,13]. In addition, the illumination is only on the front side of the solar cell.

When the solar cell is illuminated by a monochromatic light in a quasi-static regime, the incident photons that are absorbed mainly by the base, create minority carriers and some of them are recombined in the volume and at the surface area of the grain. The minority carriers' distribution in the volume of the base, is governed by the continuity equation:

$$D.\left(\frac{\partial^2\delta_n(x,y,z)}{\partial^2 x}+\frac{\partial^2\delta_n(x,y,z)}{\partial^2 y}+\frac{\partial^2\delta_n(x,y,z)}{\partial^2 z}\right)-\frac{\delta_n(x,y,z)}{\tau}=-G(z) \quad (1)$$

Where D and τ are respectively the diffusion coefficient and the average lifetime of the minority carriers; $\delta_n(x,y,z)$ is the minority carriers' density. The generation rate of the minority carriers depends on the z position and its expression can be written as follow [12,13,16] :

$$G(z)=\varnothing_0.(1-R).\alpha.e^{-\alpha.z} \quad (2)$$

Where ϕ_0 is the incident flux of photons; R is the optical reflection coefficient and α the absorption coefficient of the base. A solution of equation (1) allows us to obtain a general solution as [17,18]:

$$\delta_n(x,y,z)=\left(A.e^{\frac{-z}{L_{kj}}}+B.e^{\frac{z}{L_{kj}}}+\frac{\alpha.\varnothing_0.(1-R).L_{kj}^2.e^{-\alpha.z}}{D_{kj}\left(1-\alpha^2.L_{kj}^2\right)}\right). \quad (3)$$
$$\cos C_k.x.\cos C_j.y$$

Where, on the one hand, the coefficients C_k and C_j are determined from the following transcendent equations:

$$\tan\left(C_j.\frac{g}{2}\right)=\frac{S_g}{C_j.D} \quad (4)$$

$$\tan\left(C_k.\frac{g}{2}\right)=\frac{S_g}{C_k.D} \quad (5)$$

And on the other hand, the coefficients A and B are determined by the following boundary conditions [2] [19,20,21,22,23,24,25,26,27]:

- At the junction (emitter-base) $z=0$

$$D.\left.\frac{\partial\delta_n(x,y,z)}{\partial z}\right|_{z=0}=S_f.\delta_n(x,y,z)\Big|_{z=0} \quad (6)$$

- At the back side, $z=gz$

$$D.\left.\frac{\partial\delta_n(x,y,z)}{\partial z}\right|_{z=gz}=-S_b.\delta_n(x,y,z)\Big|_{z=gz} \quad (7)$$

Where Sg is the recombination velocity at the grain boundaries; S_b and S_f are the recombination velocities at the back side and at the junction respectively and we assume that g = gx = gy = gz.

2.1. Expression of the Photocurrent Density

The photocurrent density is obtained from the gradient of the minority carriers' density. Its expression is given as follows:

$$\mathbf{J_{ph}}=\frac{\mathbf{q.D}}{\mathbf{gx.gy}}.\int_{\frac{-gx}{2}}^{\frac{gx}{2}}\int_{\frac{-gy}{2}}^{\frac{gy}{2}}\left.\frac{\partial\boldsymbol{\delta}_n(\mathbf{x,y,z})}{\partial\mathbf{z}}\right|_{z=0}\mathbf{dx.dy} \quad (8)$$

2.2. Spectral Response (SR) Expression

The spectral response (SR) is the ratio of the photocurrent density J_{ph} to the incident power φ. Its expression is given by the equation [1] [28,29,30,31,32]:

$$SR=\frac{J_{ph}}{\varphi} \quad (9)$$

2.3. External Quantum Efficiency (EQE) Expression

The External Quantum Efficiency (EQE) is related to the spectral response by the following relation [1] [33,34,35,36]:

$$EQE=\frac{h\,C}{q\lambda}SR \quad (10)$$

With C the celerity of light; q is the elementary charge; h the Planck's constant and λ the wavelength.

3. Results and Discussions

3.1. Minority Carriers' Density Profile

The profile of the minority carriers' density according to the base depth, is shown in figure 2:

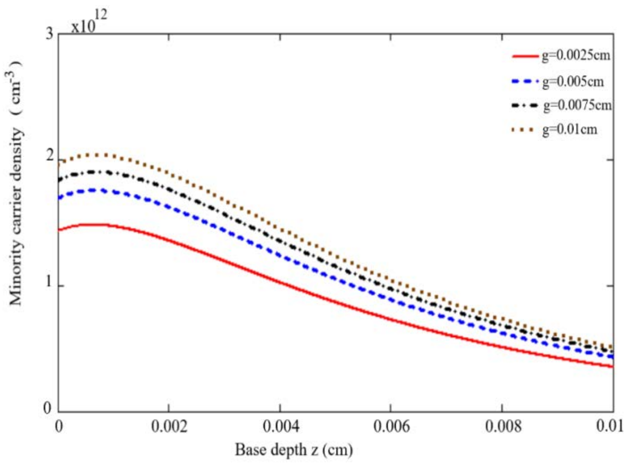

Figure 2. Minority carriers' density versus the base depth for different grain sizes With $S_g=3.10^3 cm/s$; $\lambda=0.94\mu m$; $S_f=3.10^3 cm/s$

In figure 2, for a given curve, the minority carriers' density decreases with the base depth. In the interval 0 ≤ z ≤ 0.002 cm, the density of the minority carriers is maximum in the vicinity of the junction since there is a great absorption of the incident photons that generate many minority carriers. In the interval 0.002 cm ≤ z ≤ 0.01

cm, the density of the minority carriers decreases because of a week absorption of the incident photons that is linked to a low absorption coefficient of the material: this may be due, possibly, to the recombination of the minority carriers in the volume and at the surface area of the base.

The increase in grain size leads to an increase in the amplitude of the minority carriers' density since the recombination of the minority carriers decrease at the grain boundaries and the illuminated surface of the solar cell increases.

3.2. Photocurrent Density Profile

The profile of the photocurrent density according to the junction recombination velocity is shown in figure 3:

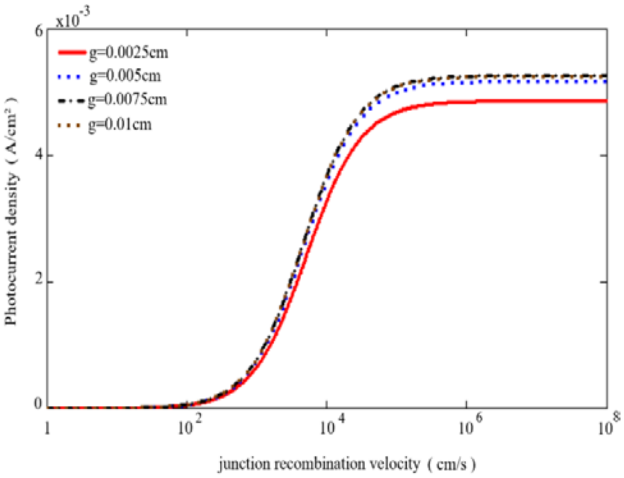

Figure 3. Photocurrent density versus the junction recombination velocity for different grain sizes With $S_g = 3.10^3 cm/s$; $\lambda = 0.94\mu m$

In figure 3, we obtain the same behavior of the curves of the photocurrent density. For a given curve, the photocurrent increases with the junction recombination. We note three zones of solar cell operating situations:

- a first zone in the interval of the junction recombination [0 cm/s; 10^2 cm/s] where the photocurrent is almost zero, in an open circuit situation. In this zone, the photogenerated minority carriers do not have enough kinetic energy to cross the junction, so they have been stored in the vicinity of the junction;

- a second zone in the interval]10^2 cm/s; 10^5 cm/s] where the operating point of the solar cell varies since the minority carriers acquire kinetic energy to cross the junction;

- a third zone in the interval]10^5 cm/s; 10^8 cm/s] where the photocurrent is maximal and corresponds to the short-circuit photocurrent: the photogenerated minority carriers have enough kinetic energy to pass through the junction.

As the grain size increases, the photocurrent density increases in amplitude since there is an increase in the photogeneration of the minority carriers in the base of the solar cell. It is noted that the variation in the amplitude of the photocurrent density with grain size is more remarkable in a short-circuit situation than that of in an open circuit situation.

3.3. Spectral Response Profile

The profile of the spectral response according to the wavelength is represented in figure 4:

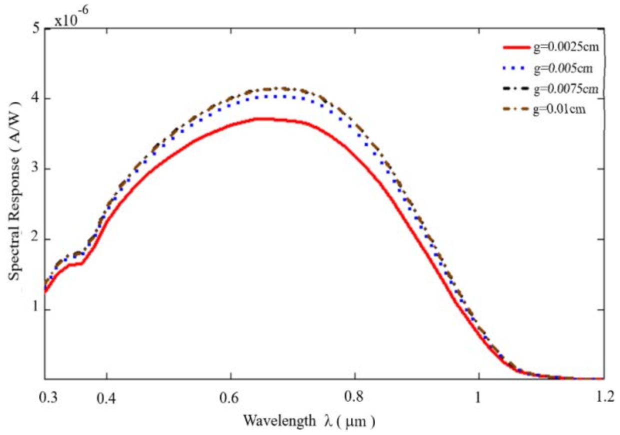

Figure 4. Spectral response versus the wavelength for different grain sizes $S_g = 3.10^3 cm/s$;

In figure 4, the spectral response is represented according to the wavelength for different grain sizes. The obtained curves have the same behavior. For a given curve, the spectral response increases with wavelength by reaching a maximum response value that corresponds to a specific wavelength λ = 0.7µm. Beyond this wavelength λ = 0.7µm, the spectral response decreases. In the wavelength range [0.3 µm ; 0.7µm], the spectral response increases because of the significant absorption of the incident photons : this is equivalent to a very good sensitivity of the solar cell. However, in the interval [0.7µm ; 1.7µm], the spectral response decreases : the base of the solar cell becomes more and more transparent to the incident light and this situation corresponds to a decrease in the sensitivity of this cell. Furthermore the increase in grain size leads to an increase in spectral response since the photogeneration of the minority carriers and the sensitivity of the solar cell increases at the same time.

3.4. External Quantum Efficiency (EQE) profile

The profile of the external quantum efficiency according to the wavelength is represented in figure 5:

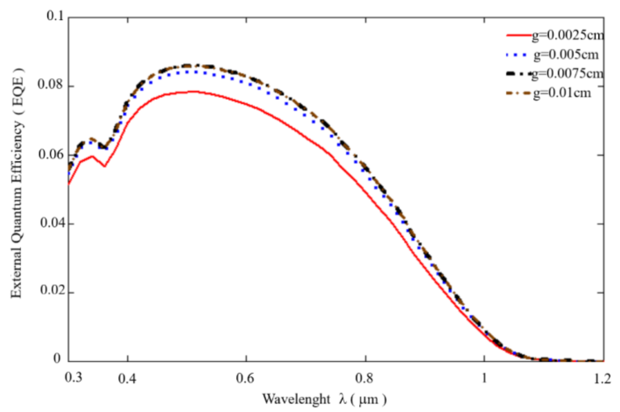

Figure 5. The profile of the external quantum efficiency in function to the wavelength

In figure 5, the quantum efficiency is represented according to the wavelength for different grain sizes. The same behavior of the four obtained curves is noted. For a given curve, the external quantum efficiency increases until reaching a maximum value that corresponds to a characteristic wavelength. For a grain size g = 0.0025 cm, we obtained the following maxima of the external quantum efficiency:

-i) the first EQE_{max1} =0.0596 corresponds to the wavelength $\lambda_1 = 0.34\mu m$;

-ii) the second EQE_{max2} =0.0783 corresponds to the wavelength $\lambda_2 = 0.5\mu m$.

For wavelengths $\lambda > \lambda_2$, the external quantum efficiency decreases since the incident photons are weakly absorbed by the base of the solar cell.

When the grain size increases, there is a change of the values of the maxima EQE_{max1} and EQE_{max2} while the wavelengths λ_1 and λ_2 obtained respectively on i) and ii) are not affected.

4. Conclusion

The profile of the photocurrent density according to the junction recombination velocity was represented. The profiles of the spectral response and the external quantum efficiency were also represented according to the wavelength for different grain sizes of a bifacial silicon solar cell. We noted that an increase of the grain size leads to a decrease of the number of the recombination centers at the grain joints that constitute negative effects of the photogenerated minority carriers and also an increase of the spectral response and the external quantum efficiency. With the wavelength $\lambda = 0.7\mu m$, the spectral response is maximum while the external quantum efficiency is maximum at $\lambda = 0,5\mu m$. In this study, we considered a fixed value of the recombination velocity at the grain boundaries and then neglected the contribution of the cell emitter. In a further works, we will take into account to the recombination velocity at the grain boundaries, the frequency modulation and an applied constant magnetic field.

ACKNOWLEDGEMENTS

We Acknowledge the Semiconductors and Solar Energy Laboratory and the Research Team in Renewable Energies, Materials and Laser for supporting this work.

References

[1] International Renewable Energy Agency, Solar Photovoltaics, Abu Dhabi, UAE, 2012.

[2] Amadou DIAO, Adama NDIAYE, Mountaga BOIRO et Senghane MBODJI “A Steady-state Spectral Response and Quantum Efficiency Determination of a Bifacial Silicon Solar Cell Under Monochromatic Illumination and Constant Magnetic Field Effects by Using the Photoconductivity Method”, American Journal of Materials Science and Engineering, 2023, Vol. 11, No. 2, pp 29-34.

[3] S. Bowden and A. Rohatgi. “Rapid and Accurate Determination and Series Resistances and Fill Factor Losses in Industrial Silicon Solar Cells”, Proceedings of the 17th European Photovoltaic Solar Energy Conference and Exhibition, Munich, Germany, pp 22-26, 2001.

[4] Luc Boussse, Shahriar Mostarshed and Dafeman. “Investigation of Carrier Transport Through Silicon Wafers by Photocurrent Measurement”. J. Appl. Phys. 75 (8), (1994), pp 4000-4008.

[5] Moustapha THIAM, Alassane DIENE, Boureima SEIBOU, Cheikh Tidiane SARR, Mohamed Lemine Ould ChEIKH, Ibrahima DIATTA, Mayoro DIEYE, Youssou TRAORE, Gregoire SISSOKO “3D Study of a Bifacial Polycrystalline Silicon Solar Cell back Surface Illuminated: Influence of Grain Size and Recombinaison Velocity”, Journal of Scientific Engineering Research, 2017, 4(1) pp 135-145.

[6] I. Ly, O. H. Lamerabott, B. Dieng, I. Gaye, S. Gueye, M. S. Diouf and G. Sissoko. “Techniques for determining recombination parameters and the domain of their validity of a polycrystalline silicon bifacial photocell under constant multispectral illumination in the static regime", Revue des énergies renouvelables Vol. 15 No 2 (2012) pp 187-206.

[7] H El Ghitani and S Martinuzzi “Influence and dislocations on electrical properties of large grained polycrystalline silicon cells I”, J. Appl. Phys, Vol 66 No 4, pp 1717-1722, 1989.

[8] M. Mbodji, B. Mbow, F. I. Barro, and G. Sissoko. “A 3D Model for thickness and diffusion capacitance of emitter-base junction determination in a bifacial polycrystalline solar cell under real operating condition”. Turking Journal of ¨Physic, 35 (2011), pp 281-290.

[9] F. I. Barro, A. Seydou Maiga, A. Wereme and G. Sissoko, “Determination of recombination parameters in the base of a bifacial silicon solar cell under constant multispectral light”. Physical and Chemical News, 56 (2010), pp 76-84.

[10] B. Ba, M. Kane, A. Fickou, G. Sissoko. “Excess minority carrier densities and transient short circuit currents in polycrystalline silicon solar cells”. Solar Energy Materials and Solar cell 31 (1993) pp 33-49.

[11] Mountaga Boiro, Amadou Diao, Adama Ndiaye, Diène Gackou, “Influence of wavelength on the Diffusion Capacitance of a serial Vertical Junction Silicon Solar Cell in Frequency Regime”, American Journal of Materials Science and Engineering, 2024, Vol 12 No.2, pp 25-29.

[12] J. Ducas “3D Modeling of a Reverse Cell Made with Improved Multicrystalline Silicon Wafer”. Solar Energy Materials and Solar Cells, 32, (1994) pp 71-88.

[13] J. Dugas and J. Oualid. “3D-Modeling of polycrystalline silicon solar cells”. Revue Phys. Appl, Vol.22. pp 677-685, (1987).

[14] Omar MBAO, Moustapha THIAM, Ibrahima LY, Ibrahima DIATTA, Marcel.S. DIOUF, Youssou TRAORE, Mor NDIAYE et Gr”goire CISSOKO, “3D Study of a polycrystalline bifacial Silicon Solar Cell, Illuminated Simultaneously by Both Sides: Grain Size and Recombinaison Velocity Influence”. International Journal of Innovative Science, Engineering and Technology, Vol. 3 Issu 12, December 2016, pp 2348-7968.

[15] M. Zoungrana, I. Zerbo, F.I. Barro, R. Sam, F. Touré, M.L. Samb and F. Zougmoré, “3-D modeling of the influence of grain size and recombination rate at grain boundaries on a polycrystalline silicon photocell under concentrated illuminance", Revue des Energies Renouvelables Vol 14 No 4, (2011) pp 649-664.

[16] Aminata GUEYE CAMARA, Ndeye THIAM, Idrissa GAYE, Sahin GÖKHAN and Grégoire SISSOKO, “3D Modeling of a Vertical Junction ¨Polycrystalline Silicon Solar Cell Under Monochromatic Illuminated in Frequency Modulation”, Current Trends in Technology and Sciences Volume: 3, Issue: 2, 2014, pp 105-107.

[17] M.C. Halder and T.R. Wiliams, “Grain boundary effects in polycrystalline silicon solar cells I: solution of the three dimensional diffusion equation by the Green’s function method”, Solar Cells, Vol.8, 1983, pp 201-223.

[18] B. Ba, M. Kane and J. Sarr, “Modelling Recombination Current in Polysilicon Solar Cell Grain Boundaries”, Solar Energy Materials and Solar Cells, Vol. 80, N°2, pp 143 – 154, 2003.

[19] M. Kunst and A. Sanders. “Transport of excess carriers in silicon Wafers”. Semicond. Sci. Technol. 7 (1992) pp 51-59.

[20] Diao A, Sissoko G, “Wavelenth and Constant Magnetic Field Dependance of the Steady-state Photoconductivity of a Bifacial Silicon Solar Cell”, Journal of Material Sciences and Engineering 2017, 6; 5.

[21] Hegedus, S. S; Shafarman, W. N; “Thin-film Solar cells: device measurement and analysis”, Prog. Photovolt. Res. Appl., 12, pp 155-176, 2004.

[22] Nzonzolo, Lilonga-Boyenga, D. Mabika, C.N and Sissoko, G. (2016). “Two-Dimensional Finite Element Method Analysis Effect of the recombinaison Velocity at the grain Boundaries on the Characteristics of a polycrystalline Silicon Solar Cell”, Circuits and Systems, 7, pp 4186-4200.

[23] S. R. Dhariwal. "Photocurrent and photovoltage from polycrystalline p-n junction solar cells". Solar Cells, Vol.25, pp 223-233, (1988).

[24] B.H. Rose and H.T. Weaver, "Determination of effective surface recombination velocity and minority carrier lifetime in high-efficiency Si solar cells", J. Appl. Phys. 54 (1983), pp 238-247.

[25] A. Dieng, N. Thiam, M. Zoungrana, S. Diallo, F.I Barro and G. Sissoko, "3-D Study of a Polycrystalline Silicon Photocell Battery: Influence of Grain Size on Electrical Parameters", Journal of Sciences, Vol. 9, N°1, pp 51-63, 2009.

[26] Mountaga BOIRO, Amadou DIAO, Adama NDIAYE, Ibrahima TOURE and Senghane MBODJI, "Influence of the Wavelength on the Series and Shunt Resistances of a Polychrystalline Silicon Solar Cell n+-p-p+ in Frequency Modulation" IRA-International Journal of Applied Sciences Vol.18, Issue 01, pp 20-31.

[27] S. MBODJI, M. DIENG, B. MBOW, F.I. BARRO, G. SISSSOKO, "Influence of grain size and grain boundary recombination velocity on the diffusion capacitance of polycrystalline bifacial silicon solar cell" Journal des Sciences pour l'Ingénieur No. 11 (2009), pp 64-69.

[28] S. Silvester, L. Sentis, and L. Castaner, "A Fast Low-Cost Solar Cell Spectral Response Measurement System With Accuracy Indicator" IEEE TRANSACTION ON INSTRUMENTATION AND MEASUREMENT, VOL. 48, No. 5, OCTOBER 1999 Engineering Environmental Sciences, Physics.

[29] Baishali Talukdar, Sukanya Buragohain, Sqnjai Kumar, V. Umakanth, Nabin Sarmah, Sadhan Mahapatra, "Effect of Spectrale Response of Solar Cell on the module Output When Individual Cell are Shaded", Solar Energy, 137 (2016) pp 303-307.

[30] Luque, A., Heggedus, S., 2011. Handbook of Photovoltaic Science and Engineering, Second Edition Jon Wiley and Sons, Ltd. ISBN: 978-0-47072169-8.

[31] Ira Devi Sara, Thomas R. Betts, Ralph Gottschalg, "Determining Spectral Response of a Photovoltaic Device Using Polychromatic Filters", IET Renewable Power Generation 2013.0248 Speciale Section : 9th Photovoltaic Science, Application and Technology Conference 2013.

[32] Martin Bliss, Alex Smit, Thomas R. Betts, Jenny Baker, Francesca De Rossi, Sai Bai, Trystan Watson, Henry Snaith, and Ralph Gottschalg, "Spectral Response Measurements of Perovskite Solar Cells", IEEE JOURNAL OF PHOTOVOLTAICS, VOL. 9, No. 1, pp 220-226, 2019.

[33] Jagdish C. Pata, Lian Lian Jiang and Douglas L. Maskell, "Estimation of External Quantum Efficiency for Multi-junction Solar Cells under Influence of Charged Particles using Artificial Neural Networks", IEE, 978-1-4577-0/11, pp 465-470, 2011.

[34] M. Boumaour, S. Sali, S. Kermadi, L. Zougar, A. Bahfir and Z. Chaieb, "High efficiency silicon solar cells with back ZnTe layer hosting IPV effect: a numerical case study", JOURNAL OF TAIBAH UNIVERSITY FOR SCIENCE, 13 (1), pp 696-703, 2019.

[35] S. Martinuzzi, I. Perichad and M. Stemmer. "External Getting around extend defects in multicrystalline silicon wafers". Solid State Phenomena, Vols. 37-38, (1994) pp 361-366.

[36] Wisnu Ananda, "External Quantum Efficiency Measurement of Solar Cell", 2017, 15th International Conference on Quality and Research (QiR): International Symposium on Electrical computer and engineering.